arXiv:cond-mat/0506736v1 [cond-mat.stat-mech] 28 Jun 2005

Topological transition in a two-dimensional model of liquid crystal

Ana I. Fariñas-Sánchez[*,**], Ricardo Paredes[*] and Bertrand Berche[*,**]

[*] *Centro de Física,*
Instituto Venezolano de Investigaciones Científicas,
Apartado 21827, Caracas 1020A, Venezuela

[**] *Laboratoire de Physique des Matériaux,*
Université Henri Poincaré, Nancy 1,
BP 239, F-54506 Vandœuvre les Nancy Cedex, France

afarinas@ivic.ve
rparedes@ivic.ve
berche@lpm.u-nancy.fr

February 6, 2008

Abstract

Simulations of nematic-isotropic transition of liquid crystals in two dimensions are performed using an $O(2)$ vector model characterised by non linear nearest neighbour spin interaction governed by the fourth Legendre polynomial P_4. The system is studied through standard Finite-Size Scaling and conformal rescaling of density profiles of correlation functions. A topological transition between a paramagnetic phase at high temperature and a critical phase at low temperature is observed. The low temperature limit is discussed in the spin wave approximation and confirms the numerical results.

PACS: 05.50.+q Lattice theory and statistics (Ising, Potts, etc.); 05.70.Jk Critical point phenomena; 64.60.Fr Equilibrium properties near critical points, critical exponents; 64.70.Md Transitions in liquid crystals.

1 Introduction

The molecules of liquid crystals may often be described by long, neutral rigid rods which interact through electrostatic dipolar or higher order multi-polar interactions. This is at the origin of the natural introduction of Legendre polynomials for the description of the orientational transition between a disordered, isotropic high temperature phase and an

ordered nematic phase at lower temperature [1]. When such a material is cooled at even lower temperatures, other ordered phases may be encountered, the description of which requires more realistic potentials (see e.g. Ref. [2]).

Lattice models of nematic-isotropic transitions capture the essentials of the above description. The molecules are represented by $n-$component unit vectors $\boldsymbol{\sigma}_{\mathbf{r}}$, hereafter called "spins", located on the sites $\mathbf{r}$ of a simple hyper-cubic lattice. The interaction between molecules is restricted to the nearest neighbours $\langle \mathbf{r}, \mathbf{r}' \rangle$, so that the radial dependence is kept constant and the angular dependence enters through a $k-$th order Legendre polynomial[1], $P_k(\cos \alpha_{\mathbf{r},\mathbf{r}'})$, where $\alpha_{\mathbf{r},\mathbf{r}'} = \widehat{(\boldsymbol{\sigma}_{\mathbf{r}}, \boldsymbol{\sigma}_{\mathbf{r}'})}$ is the angle between vectors $\boldsymbol{\sigma}_{\mathbf{r}}$ and $\boldsymbol{\sigma}_{\mathbf{r}'}$. The intensity of the interaction energy is measured through a parameter ϵ. The Hamiltonian of a lattice liquid crystal is thus given by

$$H = -\epsilon \sum_{\langle \mathbf{r},\mathbf{r}' \rangle} P_k(\cos \alpha_{\mathbf{r},\mathbf{r}'}), \tag{1}$$

and the relevant parameters for the investigation of the phase transition are the space dimension D, the "spin" dimensionality or equivalently, its symmetry $O(n)$, and the "symmetry" k of the interaction P_k.

Usual XY and Heisenberg models correspond, within this description, to $k = 1$ and $n = 2$ and 3, respectively. In two dimensions ($D = 2$), these models exhibit quite different behaviours. In the case of the XY model ($O(2)$ abelian symmetry), a topological transition described by Berezinskiĭ, and Kosterlitz and Thouless [3–5] takes place, governed by the condensation of vortices. This is not prevented by the Mermin-Wagner-Hohenberg theorem [6–8] which states that spin models with continuous symmetry cannot have any long range ordered phase. To leading order in the high-temperature expansion, one gets for the correlation function an exponential decay $\langle \boldsymbol{\sigma}_{\mathbf{r}_1} \cdot \boldsymbol{\sigma}_{\mathbf{r}_2} \rangle \sim K^{|\mathbf{r}_1 - \mathbf{r}_2|}$ ($K = \epsilon / k_B T$), while at low temperatures in the harmonic approximation, the Hamiltonian becomes quadratic and leads to the Gaussian model which implies [9] that $\langle \boldsymbol{\sigma}_{\mathbf{r}_1} \cdot \boldsymbol{\sigma}_{\mathbf{r}_2} \rangle \simeq |\mathbf{r}_1 - \mathbf{r}_2|^{-1/2\pi K}$, i.e. a temperature-dependent spin-spin critical exponent $\eta_{XY}(T) = \frac{k_B T}{2\pi\epsilon}, \quad T \to 0$. The low temperature (LT) phase of the XY model is a quasi-long-range ordered phase (QLRO) with vanishing magnetisation $M^2(T) = \lim_{|\mathbf{r}_1 - \mathbf{r}_2| \to \infty} \langle \boldsymbol{\sigma}_{\mathbf{r}_1} \cdot \boldsymbol{\sigma}_{\mathbf{r}_2} \rangle = 0$, or a critical phase. The Heisenberg model ($O(3)$, non-abelian symmetry) on the other hand has no transition at any finite temperature (asymptotic freedom) [10–13]. This difference with XY model is at first surprising, since the low temperature limit of the Heisenberg model is essentially described by a similar spin wave approximation (SWA): the longitudinal modes of the $O(n)$ model are frozen and only the transverse modes are activated, leading essentially to two Gaussian models. This apparent contradiction between the asymptotic freedom of the Heisenberg model and the topological transition at finite temperature for the XY model finds its origins in the stability of topological defects in the latter case, while the 'third spin dimension' makes the vortices unstable at any temperature in the former model. Further, the question of the accessibility of the thermodynamic limit is worth studying. Berezinskiĭ and Blank noticed long time ago that a really large, but finite XY system always possesses a *non-zero magnetisation* [14, 15]. The size being limited,

[1]Even order Legendre polynomials guarantee the local Z_2 symmetry $\boldsymbol{\sigma}_{\mathbf{r}} \to -\boldsymbol{\sigma}_{\mathbf{r}}$.

$|\mathbf{r}_1 - \mathbf{r}_2|$ becomes at most as large as the linear size L and a finite order parameter follows, $M_L(T) \sim L^{-\frac{1}{2}\eta(T)}$. More precisely, $M_L(T) = O(1)$ as long as $L \ll \mathrm{e}^{2/\eta(T)}$ a condition which can be fulfilled for any L by considering small enough temperatures. With this result in mind, we expect for the model considered hereafter that a spin wave solution will be found at low enough temperature and thus we search for an algebraic decay of the spin-spin correlation function from an effectively *non-zero* order parameter, although there is at most QLRO at low temperatures.

Changing the value of k in Eq. (1) modifies the symmetry of the spin-spin interaction and gives rise to new features[2]. When k increases, one may indeed expect a qualitative change in the nature of the transition, like in the case of discrete spin symmetries (Potts model) [18, 19]. The value $k = 2$ was intensively studied. It still corresponds to the XY model for $O(2)$ spin symmetry, while it leads to the RP^2 or Lebwohl-Lasher model [20] for $3-$component spin vectors. The nature of the transition in this latter case is still under discussion [21–25], but a recent study reported new evidences, extremely convincing, in favour of a topological transition [26]. The transition is driven by topologically stable point defects known as $\frac{1}{2}$ disclination points. Considering still larger values of k, there is a proof of asymptotic freedom in the large$-n$ limit, for values of k (in the interaction term $(1+\cos\theta)^k$) which do not exceed a critical $k_c \simeq 4.537...$ [23]. This is again discussed in a recent preprint from Caracciolo et al. [27]. Above this value the transition becomes of first order, a result which does not violate Mermin-Wagner-Hohenberg theorem, since the correlation length is finite at the transition. For finite value of n, the question of the nature of the transition at high k is still a challenging problem. In the context of orientational transitions in liquid crystals, Legendre polynomials rather than $\cos^k\theta$ interactions are introduced, and we are led to the Hamiltonian of Eq. (1). The 3-vector model with P_4 interactions was already considered in Refs. [28, 29] where convincing evidence for a first order transition was reported.

In this paper, we study the behaviour of an abelian spin model, namely $O(2)$ rotation group with P_4-like spin interactions. The model will be referred to as P_4 $O(2)$ for simplicity. We are mainly interested in the low temperature properties of the model where comparisons with analytic predictions are possible due to the simplicity of the SW approximation. The techniques used combine temperature analysis, FSS (Finite-Size Scaling) and conformal techniques (Finite-Shape Scaling - FShS - to plagiarize the famous acronym).

2 Definition of the model and of the observables

In Refs. [28, 29], the following Hamiltonian $H_{P_4\ O(3)} = -\epsilon \sum_{\langle \mathbf{r},\mathbf{r}'\rangle} P_4(\boldsymbol{\sigma}_\mathbf{r} \cdot \boldsymbol{\sigma}_{\mathbf{r}'})$ was considered, where $\boldsymbol{\sigma}_\mathbf{r} = (\sigma^x_\mathbf{r}, \sigma^y_\mathbf{r}, \sigma^z_\mathbf{r})$, $|\boldsymbol{\sigma}_\mathbf{r}| = 1$ and $P_4(x) = \frac{1}{8}(35x^4 - 30x^2 + 3)$. For $2-$component vectors, in the completely disordered phase $\langle\cos^2\theta\rangle = \frac{1}{2}$ and $\langle\cos^4\theta\rangle = \frac{3}{8}$. In order to keep the same symmetry in the interaction than in the P_4 $O(3)$ model, but to normalise it between 0 and 1 in the limits of completely disordered and completely ordered phases

[2] In the same spirit, the case of symmetry-breaking magnetic fields $h_k \cos k\theta$ added to the XY model and changing the phase diagram was investigated by José et al [16, 17].

respectively, we modify slightly the Hamiltonian to include pair interactions of the type $Q_4(x) \equiv AP_4(x) + \text{const} = \frac{8}{55}(35x^4 - 30x^2 + \frac{15}{8})$. The corresponding Hamiltonian is thus defined by

$$H_{P_4\ O(2)} = -\epsilon \sum_{\langle \mathbf{r},\mathbf{r}' \rangle} Q_4(\boldsymbol{\sigma}_\mathbf{r} \cdot \boldsymbol{\sigma}_{\mathbf{r}'}), \tag{2}$$

with now $\boldsymbol{\sigma}_\mathbf{r} = (\sigma^x_\mathbf{r}, \sigma^y_\mathbf{r})$, $|\boldsymbol{\sigma}_\mathbf{r}| = 1$. A qualitative description of the transition is provided by the temperature behaviour of the energy density, the specific heat, the order parameters and the corresponding susceptibilities. The internal energy is defined from the thermal average of the Hamiltonian density,

$$u_{P_4\ O(2)}(T) = (DL^D)^{-1} \langle H_{P_4\ O(2)} \rangle \tag{3}$$

and the specific heat follows from fluctuation dissipation theorem,

$$L^D T^2 C_v(T) = \langle (H_{P_4\ O(2)})^2 \rangle - \langle H_{P_4\ O(2)} \rangle^2. \tag{4}$$

Brackets denote the thermal average. The definition of the scalar order parameter (sometimes called nematisation) is deduced from the local second-rank order parameter tensor,

$$q^{\alpha\beta}(\mathbf{r}) = \sigma^\alpha_\mathbf{r} \sigma^\beta_\mathbf{r} - \frac{1}{2}\delta^{\alpha\beta}. \tag{5}$$

After space average, the traceless tensor $L^{-D} \sum_\mathbf{r} q^{\alpha\beta}(\mathbf{r})$ admits two opposite eigenvalues $\pm\frac{1}{2}\eta$ corresponding to eigenvectors $\mathbf{n}_+$ and $\mathbf{n}_-$. The order parameter density is defined after thermal averaging by

$$q_2(T) = \langle \eta \rangle. \tag{6}$$

This quantity has the same physical content but is more stable numerically than a direct estimation of $\langle 2(\boldsymbol{\sigma}_\mathbf{r} \cdot \mathbf{n}_+)^2 - 1 \rangle$. Another order parameter may be defined simply by inspection of the structure of the Hamiltonian,

$$q_4(T) = L^{-D} \langle \sum_\mathbf{r} Q_4(\boldsymbol{\sigma}_\mathbf{r} \cdot \mathbf{n}_+) \rangle. \tag{7}$$

The associated susceptibilities are defined by the fluctuations of the order parameter densities, e.g.

$$\chi_{q_2}(T) = \frac{4L^D}{k_B T} (\langle \eta^2 \rangle - \langle \eta \rangle^2). \tag{8}$$

3 Thermal behaviour

In this section, we illustrate the behaviour of the various thermodynamic quantities as the temperature varies. It gives a *first idea* of the nature of the transition.

The simulations are performed using a standard Wolff algorithm suited to the expression of the nearest neighbour interaction [29, 30]. The spins are located on the vertices of a simple square lattice of size L^2 with periodic boundary conditions in the two directions. We use $L = 24$, 32, 48, 64 and 128 with 10^6 equilibrium steps (measured as the number

of flipped Wolff clusters) and 10^6 Monte Carlo steps (MCS) for the evaluation of thermal averages. The autocorrelation time (at $k_BT/\epsilon = 0.2$, $L = 16$) is of order of 30 MCS, hence the numbers of iterations that we used correspond roughly to 3.10^4 independent measurements for the smallest size and is still safe at $L = 128$.

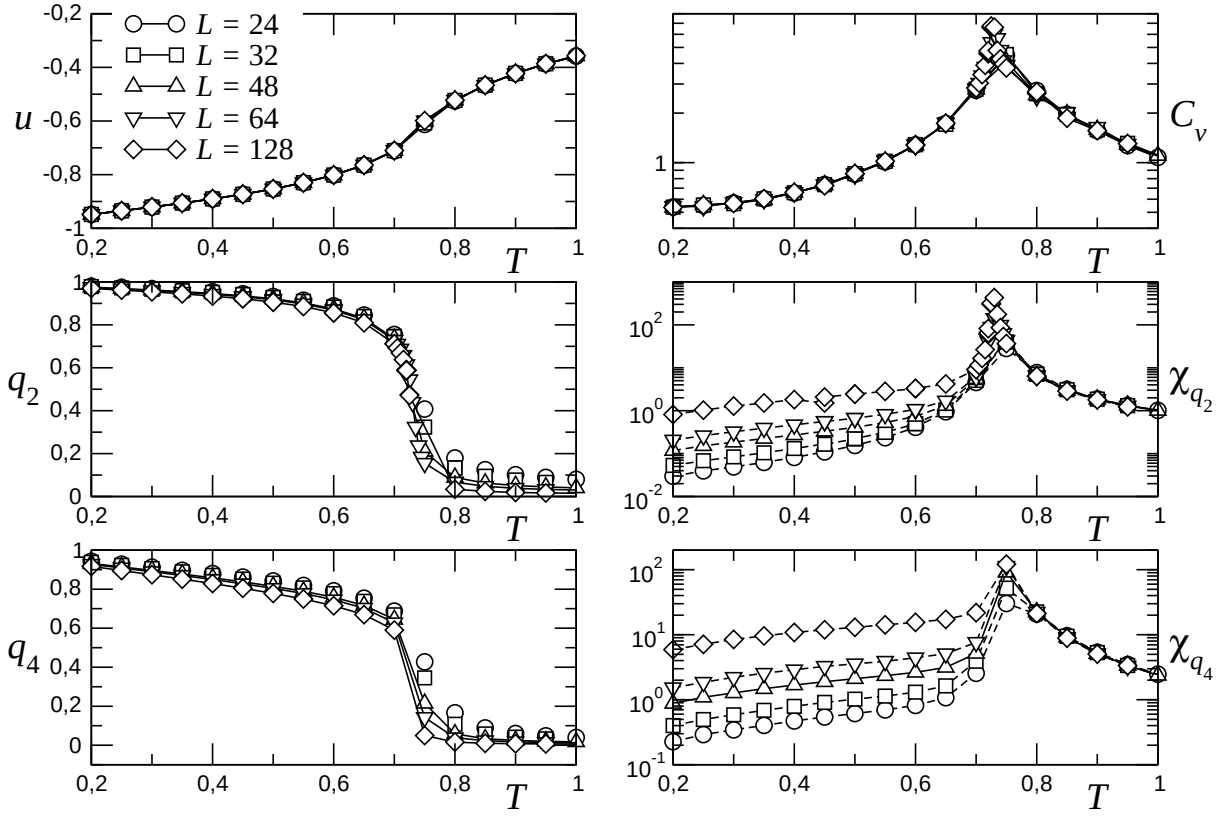

Figure 1: Energy, specific heat, order parameter q_2 and corresponding susceptibility χ_{q_2}, order parameter q_4 and corresponding susceptibility χ_{q_4} vs T for the P_4 $O(2)$ model. The full lines are only guides for the eyes. The values of k_B and ϵ have been fixed to unity.

We deliberately did not use histogram reweighting which would require a huge amount of simulation time to be reliable. We have adopted a different strategy here, producing more simulations with less iterations, but with a better control of the errors than at the ends of the histograms. The temperature dependence of thermodynamic quantities is plotted in Fig. 1 for different system sizes. The behaviour of the energy density clearly displays a difference between the regimes of low and high temperatures. This is the signature of a transition and this naive statement is corroborated by the behaviours of the other physical quantities, the specific heat C_v, the order parameters q_2 and q_4, and the corresponding susceptibilities. The specific heat close to the maximum does not seem to increase substantially with the system size. This might be the sign of an essential singularity [3] around a temperature $k_BT_c/\epsilon \simeq 0.70 - 0.75$. From the behaviour

[3]Or at least the sign of a non diverging specific heat with non-positive exponent α.

of the order parameters, we may suspect a smooth transition, since there is no sharp jump. The susceptibilities display a non conventional behaviour at low temperature, increasing with the system size, which indicates a likely topological transition with a critical low temperature phase where the susceptibility diverges at any temperature (note the logarithmic scale for vertical axis).

The probability distributions of the energy density and the order parameter is also instructive. Both quantities are shown in Fig. 2. The distributions have a simple shape with single peaks, and this is still true for temperatures below the transition, a result which suggests a continuous transition. We note that due to the finite-size of the system, the order parameter is finite.

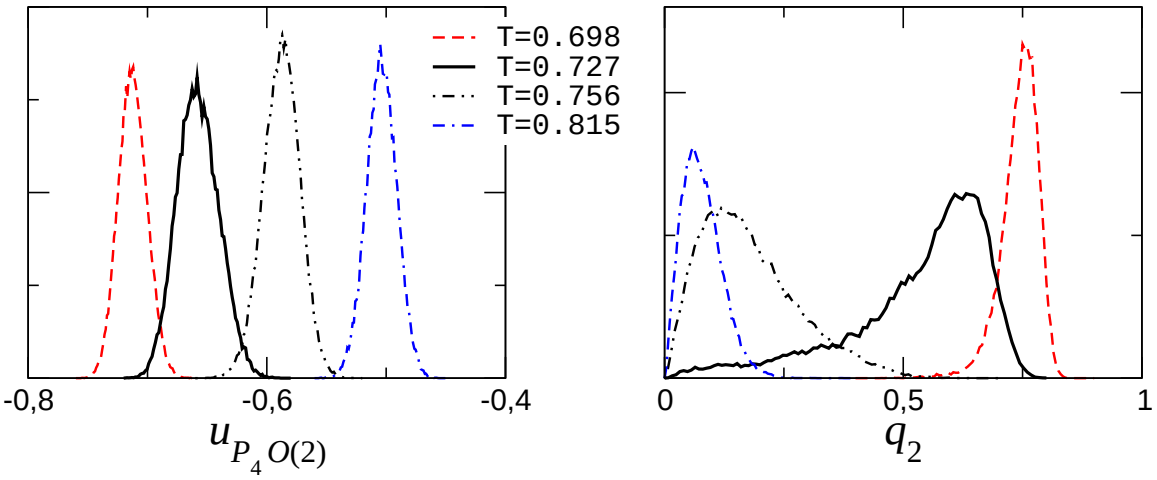

Figure 2: Energy density and order parameter probability distributions (arbitrarily normalized) for the P_4 $O(2)$ model at a temperature close to the transition . The system size is $L = 48$ and the temperatures are given in units suche that $k_B/\epsilon = 1$. The solid lines correspond to the effective transition.

4 Finite-Size Scaling

In this section we investigate the properties of the low temperature phase using Finite-Size Scaling technique. In the critical low temperature phase of a model which displays a topological transition (the paradigmatic XY model serves as a guide), the physical quantities behave like at criticality for a second-order phase transition, with power law behaviours of the system size. The difference is that in the critical phase, the critical exponents depend on the temperature and for any temperature below the transition one has e.g.

$$q_2(T) \sim L^{-\frac{1}{2}\eta_{q_2}(T)} \tag{9}$$

$$\chi_{q_2}(T) \sim L^{2-\eta_{q_2}(T)}. \tag{10}$$

Here $\eta_{q_2}(T)$ denotes the correlation function critical exponent, defined by

$$\langle Q_2(\cos(\theta_{\mathbf{r}_1} - \theta_{\mathbf{r}_2}))\rangle \sim |\mathbf{r}_1 - \mathbf{r}_2|^{-\eta_{q_2}(T)}. \tag{11}$$

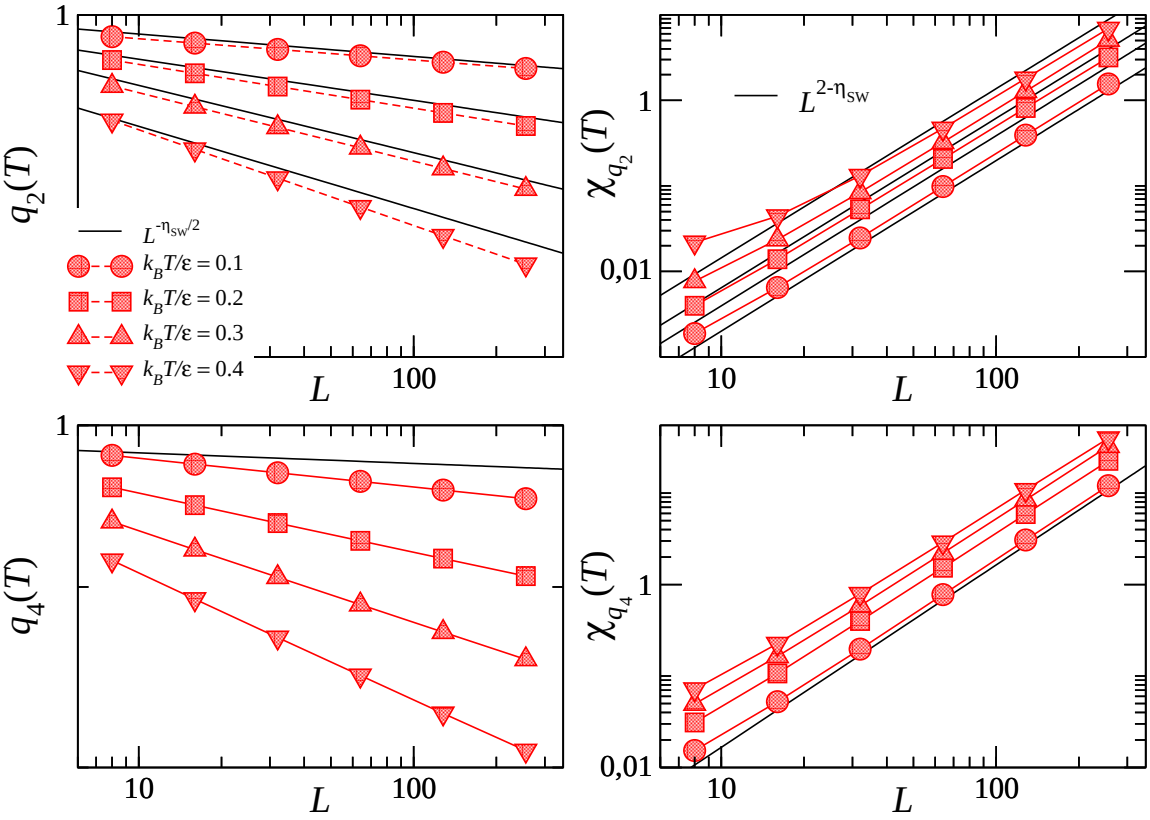

Figure 3: FSS behaviour of the order parameter densities $q_2(T)$ and $q_4(T)$ and the corresponding susceptibilities for the P_4 $O(2)$ model at temperatures $k_BT/\epsilon = 0.1$, 0.2 and 0.4 below the transition temperature. Temperature-dependent exponents are confirmed and the full lines show the expected SW result which nicely fits the data at low temperatures.

In Fig. 3 the FSS behaviour of the order parameter densities and of the corresponding susceptibilities is shown on log-log scales vs the system size L (we used $L = 16$, 32, 48, 64, 128 and 256) for different values of T below the expected transition. The linear behaviour on this scale indicates power laws, and the different slopes at different temperatures is the result of exponents which depend on the value of the temperature. Starting from a fully ordered system at $T = 0$, at low temperature we can expect a small disorientation of the molecules and the spin-wave approximation becomes correct. For $O(2)$ model with nearest neighbour interactions described by arbitrary polynomial in $\cos\alpha_{\mathbf{r},\mathbf{r}'}$, one is led to an effective harmonic Hamiltonian $\frac{1}{2}\epsilon\sum_{\langle\mathbf{r},\mathbf{r}'\rangle} l(\theta_{\mathbf{r}} - \theta_{\mathbf{r}'})^2$. It yields power-law correlations,

$$\langle\cos m(\theta_{\mathbf{r}_1} - \theta_{\mathbf{r}_2})\rangle = \mathrm{e}^{-\frac{m^2}{2}\langle(\theta_{\mathbf{r}_1} - \theta_{\mathbf{r}_2})^2\rangle} \sim |\mathbf{r}_1 - \mathbf{r}_2|^{-\eta_{ml}^{\mathrm{SW}}} \tag{12}$$

with a spin-wave decay exponent given by

$$\eta_{ml}^{\rm SW} = \frac{m^2}{l}\eta_{XY}(T) = \frac{m^2 k_B T}{2l\pi\epsilon}. \tag{13}$$

This expression, if confirmed numerically, will support the presence of a quasi-long-range ordered, scale-invariant phase at low temperatures. The exponent $\eta_{q_2}(T)$ ($m = 2$) is accessible through $q_2(T)$ (or the corresponding susceptibility) via equations (9) and (10). We note that it is also accessible through the the FSS behaviour of $q_4(T)$, since the leading behaviour of $\langle Q_4(\theta_{\mathbf{r}_1} - \theta_{\mathbf{r}_2})\rangle$ is still governed by $\langle \cos 2(\theta_{\mathbf{r}_1} - \theta_{\mathbf{r}_2})\rangle$. In Fig 3, one may extract numerical values of η exponent. The values $\eta_{q_2}(T) = 0.0056$, 0.0117, 0.0182, and 0.0256 are obtained at $k_B T/\epsilon = 0.1$, 0.2, 0.3, and 0.4, respectively. Using the small angle limit $H_{P_4\ O(2)} = -\epsilon \sum_{\langle \mathbf{r},\mathbf{r}'\rangle} Q_4(\cos\alpha_{\mathbf{r},\mathbf{r}'}) \simeq \frac{1}{2}\epsilon \sum_{\langle \mathbf{r},\mathbf{r}'\rangle} \frac{128}{11}(\theta_{\mathbf{r}} - \theta_{\mathbf{r}'})^2$, we have $l = \frac{128}{11}$ which yields $\eta_{2\frac{128}{11}}^{\rm SW} = \frac{11 k_B T}{64\pi\epsilon}$. At $k_B T/\epsilon = 0.1$, 0.2, 0.3, and 0.4, we get $\eta_{2\frac{128}{11}}^{\rm SW}(T) \simeq 0.006$, 0.011, 0.018, and 0.022 which confirm the numerical values, since the SW exponent is always a lower bound for the exact exponent $\eta_{q_2}(T)$. The comparison is made visible in the figure where the SW values are plotted in full lines while the symbols represent the numerical data. As expected, the lower the temperature, the better the SW approximation.

5 Finite-Shape Scaling

Inspired by the results that we obtained for the Lebwohl-Lasher model [24] or the XY model [31–33], we will now produce a complementary study using a rescaling of the density profiles. For that purpose, we assume the existence of a critical phase at low temperatures as suggested by the temperature dependence and FSS results. If the assumption is revealed incorrect, we will be led to some inconsistency.

The existence of a scale-invariant low temperature critical phase leads to conformally covariant density profiles or correlation functions at *any temperature below the transition* T_c. It is then advantageous to deduce the functional expression of the correlation functions or density profiles in a restricted geometry adapted to numerical simulations from a conformal mapping $w(z)$:

$$G(w_1, w_2) = |w'(z_1)|^{-x_\sigma} |w'(z_2)|^{-x_\sigma} G(z_1, z_2) \tag{14}$$

Here, w labels the lattice sites in the transformed geometry (the one where the computations are really performed), z is the corresponding point in the original one (usually the infinite plane where the two-point correlations take the standard power-law expression $G(z_1, z_2) \sim |z_1 - z_2|^{-\eta_\sigma}$), and $x_\sigma = \frac{1}{2}\eta_\sigma$ is the scaling dimension associated to the scaling field under consideration. The interest of such an approach lies in the full inclusion of the changes due to shape effects in the functional expression and we may copy the terminology FSS and call it *Finite-Shape Scaling*. Rather than two-point correlation functions, it is even more convenient to work with density profiles $m(w)$ in a finite system with symmetry breaking fields along some surfaces in order to induce a non-vanishing local order parameter in the bulk. The density $m(w)$ will be $q_2(\mathbf{r}) = \langle Q_2(\boldsymbol{\sigma}_{\mathbf{r}} \cdot \mathbf{h}_{\partial\Lambda})\rangle$ or higher

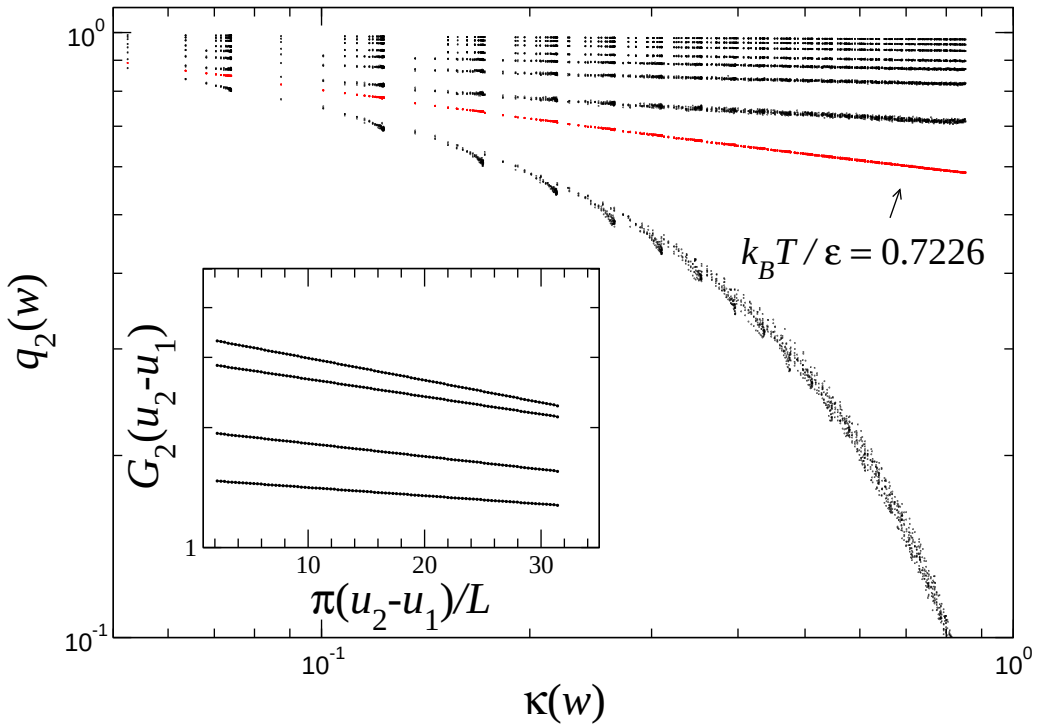

Figure 4: Finite-Shape Scaling behaviour ($L = 64$) of the order parameter density profile $q_2(w)$ for various temperatures k_BT/ϵ below the transition temperature and one temperature above. The transition takes place around the value 0.70. The insert shows (on a semi-log scale) the exponential decay of correlation function (below the transition) along a torus as explained in the text.

rank nematisation $q_4(\mathbf{r}) = \langle Q_4(\boldsymbol{\sigma}_\mathbf{r} \cdot \mathbf{h}_{\partial\Lambda})\rangle$. In the case of a square lattice Λ of size $L \times L$, with fixed boundary conditions along the four edges $\partial\Lambda$, one expects

$$\begin{aligned} m(w) &\sim [\kappa(w)]^{-\frac{1}{2}\eta_\sigma} \\ \kappa(w) &= \Im\mathrm{m}\left[\mathrm{sn}\frac{2\mathrm{K}w}{L}\right] \times \left|\left(1-\mathrm{sn}^2\frac{2\mathrm{K}w}{L}\right)\left(1-k^2\mathrm{sn}^2\frac{2\mathrm{K}w}{L}\right)\right|^{-\frac{1}{2}} \end{aligned} \tag{15}$$

where w stands for lattice site $\mathbf{r}$. This expression easily follows from the expression of the order parameter profile decaying in the upper half-plane from a distant surface of spins constantly fixed in a given direction, $m(z) \sim y^{-x_\sigma}$, and from the conformal transformation of the upper half-plane $z = x + iy$, $(0 \le y < \infty)$, inside a square $w = u + iv$ of size $L \times L$, $(-L/2 \le u \le L/2, 0 \le v \le L)$, with open boundary conditions along the four edges, realized by a Schwarz-Christoffel transformation

$$w(z) = \frac{L}{2\mathrm{K}}\mathrm{F}(z,k), \qquad z = \mathrm{sn}\left(\frac{2\mathrm{K}w}{L}\right). \tag{16}$$

Here, $\mathrm{F}(z,k)$ is the elliptic integral of the first kind, $\mathrm{sn}(2\mathrm{K}w/L)$ the Jacobian elliptic sine, $\mathrm{K} = \mathrm{K}(k) = \mathrm{F}(1,k)$ the complete elliptic integral of the first kind, and the modulus $k = 0.171573$ depends on the aspect ratio of Λ (here 1).

The procedure is now to fit numerical data of the order parameter profile against expression (15). The result for the density profile of $q_2(w)$ is shown on a log-log scale in Fig. 4. At low temperatures, the resulting straight lines confirm the existence of a critical phase (a linear behaviour on this scale results from an algebraic decay in the original semi-infinite geometry). Above the deconfining transition (assuming that it is indeed the driving mechanism of the transition), the decay becomes faster, indicating a paramagnetic phase. The transition is approximately located at a temperature $k_B T_c/\epsilon \simeq 0.70 - 0.75$. The scenario is eventually completely consistent with a BKT transition. Furthermore the η exponent again follows from the scaling of the density profile in Eq. (15) which provides an alternate determination of this quantity.

Another famous conformal mapping which has been applied to many two-dimensional critical systems is the logarithmic transformation $w(z) = \frac{L}{2\pi} \ln z = \frac{L}{2\pi} \ln \rho + i \frac{L\varphi}{2\pi}$. It maps the infinite plane onto an infinitely long cylinder of perimeter L, and due to the one-dimensional character of this latter geometry, the correlation functions along the axis of the cylinder (let say in terms of the variable $u = \frac{L}{2\pi} \ln \rho$) decay exponentially at criticality, $G(u_1, u_2) \sim \exp[-(u_2 - u_1)/\xi]$. The interesting result which makes this technique powerful is that the correlation length amplitude on the strip is universal and only determined by the corresponding η exponent, $\xi = \frac{L}{\pi\eta}$. This relation is known as the gap-exponent relation in the context of quantum chains in $1 + 1$ dimensions. It was conjectured by several authors [34–36] before Cardy proved it [37]. Using MC simulations we cannot of course produce an infinitely long cylinder. It is however possible to perform simulations inside a rectangle $L_1 \times L$ with $L_1 \gg L$ and periodic boundary conditions in both space directions (we get a very long torus). Due to the exponential decay of the correlation length, it is not necessary to explore really long distances $u_2 - u_1$ (typically $u_2 - u_1 \leq 10L$). A finite torus of long perimeter $10^3 L$ thus only produces insignificant finite-size corrections to the gap-exponent relation. We performed the simulations at different temperatures in a system of size 10×10000 and extracted the correlation function exponent from the linear behaviour

$$\ln \langle Q_2[\cos(\theta_{u_2} - \theta_{u_1}]\rangle = \text{const} - \frac{\pi \eta_{q_2}}{L}(u_2 - u_1). \tag{17}$$

This linear behaviour (in terms of the variable $u_2 - u_1$) is shown in the insert of Fig. 4 where for simplicity $\langle Q_2[\cos(\theta_{u_2} - \theta_{u_1}]\rangle$ is denoted $G_2(u_2 - u_1)$. It is impossible to apply this technique up to the transition temperature, since the strip system contains quite a large number of spins (10^5 while simulations in the square geometry are performed up to typically 10^4 spins) and the autocorrelation time increases too fast.

6 Behaviour at the deconfining transition

Not only the low temperature behaviour is interesting. The value of the η exponent at the BKT transition where some deconfining mechanism should lead to the proliferation of unbinded topological defects is also of primary interest. For that purpose, an accurate value of the transition temperature is needed. We performed a study of the crossing of U_4 Binder cumulant for very large statistics (30×10^6 MCS) and large system sizes (squares

: results shown in Fig. 5

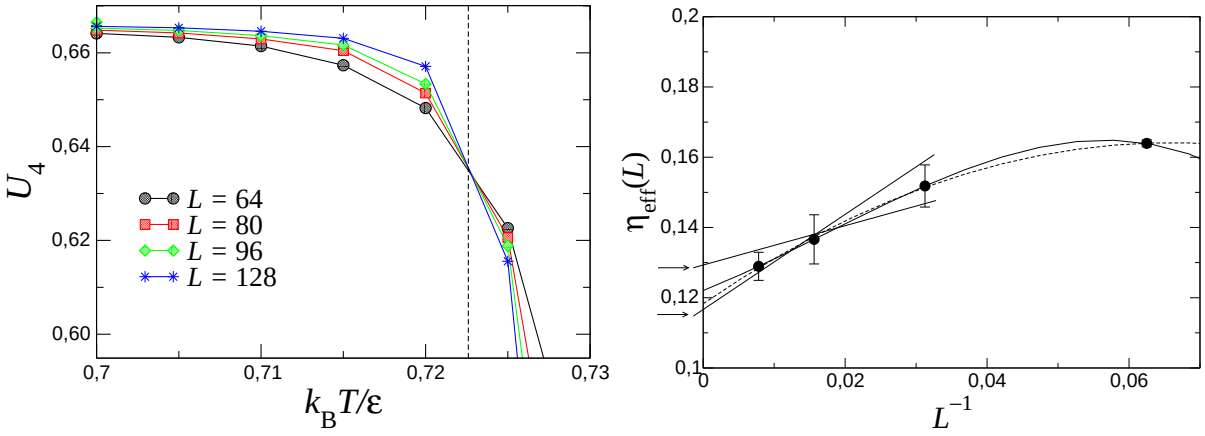

Figure 5: Left: Crossing of the Binder parameter at the deconfining transition at a temperature $k_B T_{\rm BKT}/\epsilon = 0.7226$. Right: Size dependence of the correlation function exponent at $T_{\rm BKT}$ ($L = 16$, 32, 64, 128) and extrapolation to the thermodynamic limit.

Then this temperature is used to perform Finite-Shape Scaling using the technique already employed for the investigation of the low temperature phase, namely the algebraic decay of density profiles inside a square with fixed bounday conditions. These new simulations are really time-consuming, since the autocorrelation time increases in the low temperature phase when T evolves towards the deconfining transition and a rather large number of Monte Carlo steps is needed to get a satisfying number of independent measurements. For sizes $L = 16$, 32, 64, we used 10^6 MCS for thermalization and 30.10^6 for measurements, while "only" 20.10^6 for the largest size 128. For technical reasons, the exponential decay of two-point correlation functions along the torus cannot be applied at the BKT transition, since as already mentioned the system size being quite larger than in a square geometry, the number of MC iterations required is by far too large. In Fig. 5 we plot the "effective" exponent $\eta_{\rm eff}(L)$ measured at $T_{\rm BKT}$ for different system sizes as a function of the inverse size. An estimate of the thermodynamic limit value ($L \to \infty$) can be made using a polynomial fit (the results of quadratic and cubic fits are respectively 0.118 and 0.122). It is safer to keep the three largest sizes available, $L = 32$, 64, and 128, for which a linear dependence of $\eta_{\rm eff}(L)$ with L^{-1} is observed. Taking into account the error bars, crossing the extreme straight lines leads to the following value for the correlation function exponent at the deconfining transition

$$\eta_{q_2}(T_{\rm BKT}) = 0.122 \pm 0.007. \tag{18}$$

This value is essentially half the Kosterlitz value for the XY model.

7 Conclusion

In Fig. 6 we plot as a function of the temperature the exponent $\eta_{q_2}(T)$ measured after conformal rescaling of the density profile and correlation functions at different system sizes and the FSS determination which follows from Fig. 3. Together with the exponent determined numerically, we report the result of the spin-wave approximation, shown in dotted line. The larger the size of the system, the better the agreement. Similar results (not shown here) are measured in the case of the higher-order nematisation, $q_4(T)$.

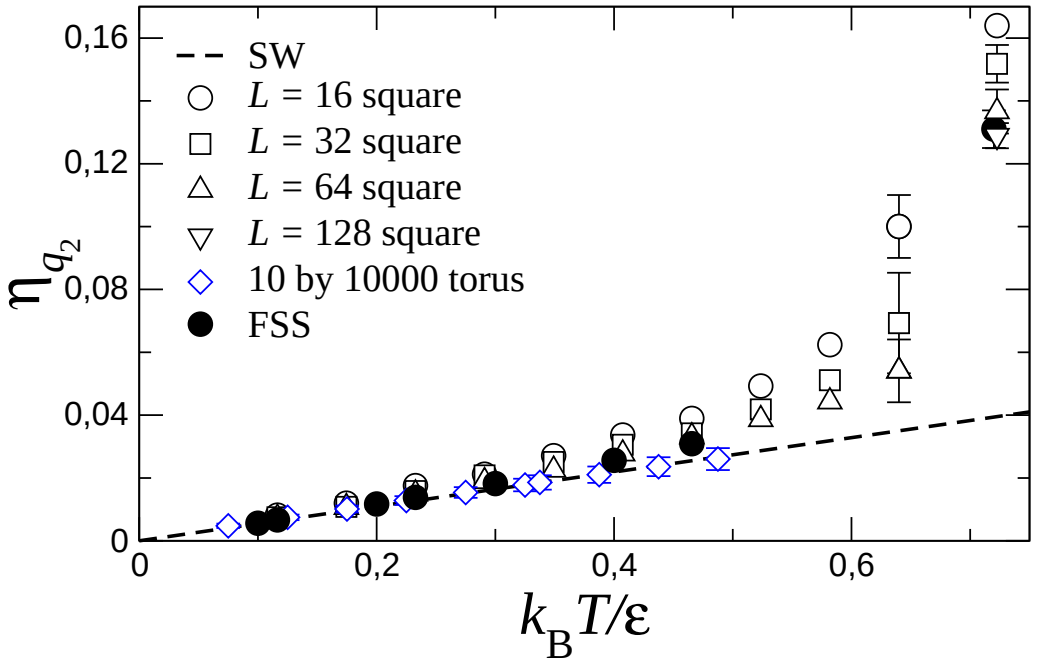

Figure 6: Temperature variation of the correlation function exponent $\eta_{q_2}(T)$ deduced from conformal rescaling (open symbols) and FSS (filled symbols). Open triangles and diamonds, which correspond the largest systems where we appplied FShS seem quite reliable. The dashed lines shows the result of the spin-wave approximation $\eta_{q_2}(T) = \eta_{2\frac{128}{11}}^{(2)} = \frac{11}{64}\frac{k_B T}{\pi\epsilon}$.

According to these results, the main outcome of the present work is the following:

- P_4 $O(2)$ model displays a BKT-like transition with QLRO in the LT phase where SWA nicely fits the nematisation temperature-dependent exponent $\eta_{q_2}(T)$ when $T \to 0$.

The LT phase of the model is thus disordered. Nevertheless, in what we will call a *physical limit*, i.e. a finite but quite large size where the system contains a macroscopic number of spins, it is useful to consider that the system is partially ordered, as Fig. 2 seems to indicate.

These results find a partial interpretation through a naive comparison with clock model in 2D. Increasing the order of the interaction polynomial indeed increases the number of

deep wells which stabilise the relative orientation of neighbouring spins. One is thus led to a system which is quite similar to a planar clock model with a finite number of states, unless the fact that here we keep a continuous spin symmetry which prevents from any "magnetic" long-range order at finite temperature. The clock model is known to be in the Potts universality class when $q = 3$, but at $q \geq 4$, it displays a QLRO phase before conventional ordering at lower temperatures [16]. Combining these results with the requirements of Mermin-Wagner-Hohenberg theorem in the case of continuous spin symmetry gives a natural framework for the comprehension of our results for $2-$component spin systems. Whatever the nearest-neighbour interaction (in P_1, P_2 or P_4) their behaviour seems to be always described by a BKT transition. The similar observation that a two-component nematic model renormalises in two dimensions towards the XY model was already reported in Ref. [38]. The transition is likely driven by a mechanism of condensation of defects, like in the XY model, but due to the local Z_2 symmetry not only usual vortices carrying a charge ± 1 are stable, but also disclination points carrying charges $\pm 1/2$ should be stable. The role of these defects might be studied in a similar way than in the recent work of Dutta and Roy [26], by the comparison of the the transition in the pure model and in a modified version where a chemical potential is artificially introduced in order to control the presence of defects.

Acknowledgement

The work of A.I.F.S. is supported by a PCP cooperation programme ("*Fluides pétroliers*") between France and Venezuela. Thanks to the support from CINES in Montpellier for computational time. We benefited from instructive correspondence on $O(n)$ models with H. Kawamura, A. Pelissetto, D. Mouhanna and S. Korshunov who are gratefully acknowledged. B.B. is also indebted to Yu. Holovatch for stimulating discussions at the occasion of one of his visits in Nancy.

References

[1] W. Maier and A. Saupe, *Z. Naturforsch.* **14A**, 882 (1959).

[2] H. Zewdie, *Bull. Chem. Soc. Ethiop.* **14**, 69 (2000).

[3] V.L. Berezinskiĭ , *Sov. Phys. JETP* **32**, 493 (1971).

[4] J.M. Kosterlitz and D.J. Thouless, *J. Phys. C: Solid State Phys.* **6**, 1181 (1973).

[5] J.M. Kosterlitz, *J. Phys. C: Solid State Phys.* **7**, 1046 (1974).

[6] N.D. Mermin and H. Wagner, *Phys. Rev. Lett.* **22**, 1133 (1966).

[7] P.C. Hohenberg, *Phys. Rev.* **158**, 383 (1967).

[8] A. Gelfert and W. Nolting, *J. Phys. Condens. Matter* **13**, R505 (2001).

[9] T.M. Rice, *Phys. Rev.* **140**, A 1889 (1965).

[10] A.M. Polyakov, *Phys. Lett.* **59B**, 79 (1975).

[11] E. Brézin and J. Zinn-Justin, *Phys. Rev. B* **14**, 3110 (1976).

[12] D.J. Amit, Field theory, the renormalization group and critical phenomena, World Scientific, Singapore 1984.

[13] Yu.A. Izyumov and Yu.N. Skryabin, Statistical mechanics of magnetically ordered systems, Kluwer Academic Publishers, New-York 1988.

[14] V.L. Berezinskiĭ and A. Ya. Blank, *Sov. Phys. JETP* **37**, 369 (1973).

[15] S.T. Bramwell and P.C.W. Holdsworth, *J. Phys. Condens. Matter* **5**, L53 (1993).

[16] J.V. José, L.P. Kadanoff, S. Kirkpatrick and D.R. Nelson, *Phys. Rev. B* **16**, 1217 (1977).

[17] D.R. Nelson, Defects and geometry in condensed matter physics, Cambridge University Press, Cambridge 2002.

[18] E. Domany, M. Schick and R.H. Swendsen, *Phys. Rev. Lett.* **52**, 1535 (1984).

[19] A. Jonsson, P. Minnhagen and M. Nylén, *Phys. Rev. Lett.* **70**, 1327 (1993).

[20] P.A. Lebwohl and G. Lasher, *Phys. Rev. A* **6**, 426 (1973).

[21] H. Kunz and G. Zumbach, *Phys. Rev. B* **46**, 662 (1992).

[22] H.W.J. Blöte, W. Guo and H.J. Hilhorst, *Phys. Rev. Lett.* **88**, 047203 (2002).

[23] S. Caracciolo and A. Pelissetto, *Phys. Rev. E* **66**, 016120 (2002).

[24] A.I. Fariñas-Sánchez, R. Paredes and B. Berche, *Phys. Lett. A* **308**, 461 (2003).

[25] R. Paredes, A.I. Fariñas-Sánchez and B. Berche, cond-mat/0401457.

[26] S. Dutta and S.K. Roy, *Phys. Rev. E* **70**, 066125 (2004).

[27] S. Caracciolo, B.M. Mognetti and A. Pelissetto, cond-mat/0409536.

[28] K. Mukhopadhyay, A. Pal and S.K. Roy, *Phys. Lett. A* **253**, 105 (1999).

[29] A. Pal and S.K. Roy, *Phys. Rev. E* **67**, 011705 (2003).

[30] U. Wolff, *Phys. Rev. Lett.* **62**, 362 (1989).

[31] B. Berche, A.I. Fariñas Sanchez and R. Paredes V., *Europhys. Lett.* **60**, 539 (2002).

[32] B. Berche, *J Phys. A* **36**, 585 (2003).

[33] B. Berche and L.N. Shchur, *Pis'ma v ZhETF* **79**, 267 (2004), *JETP Lett.* **79**, 213 (2004).

[34] J.L. Pichard and G. Sarma, *J. Phys. C* **14**, L127 (1981).

[35] B. Derrida and L. de Seze, *J. Physique* **43**, 475 (1982).

[36] J.M. Luck, *J. Phys. A* **15**, L169 (1982).

[37] J.L. Cardy, *J. Phys. A* **17**, L385 (1984).

[38] D.R. Nelson and R.A. Pelcovits, *Phys. Rev. B* **16**, 2191 (1977).